SOURCE ARRAY ANALYSIS ON THE COMPOSITION OF REGIONAL WAVES FROM BALAPAN EXPLOSIONS IN THE NEAR-SOURCE REGION

Tae-Kyung Hong and Jiakang Xie

Lamont-Doherty Earth Observatory of Columbia University

Sponsored by National Nuclear Security Administration
Office of Nonproliferation Research and Engineering
Office of Defense Nuclear Nonproliferation

Contract No. DE-FC52-03NA99514

ABSTRACT

Regional seismic waves from 67 historic underground nuclear explosions (UNEs) in the Balapan test site of Kazakhstan, recorded at station Borovoye (BRV), are studied with a source array analysis under the reciprocity theorem. The source array data are used to conduct a frequency-slowness power spectra (FSPS) analysis to determine the phase composition of the plane wave fields in the near source region. Since station BRV is equipped with short-period instruments with flat displacement responses above 1 hz, our analysis is limited to high-frequencies above about 0.5 Hz. Source locations and the origin times are obtained from geodetic measurements, a scaling law between event magnitudes and depths, and a calibrated Pn travel time curve. Between frequencies of 0.5 and 3.0 Hz, the *Pn* slowness power spectra are concentrated at a phase velocity (v_h) of 8.0 km/s. The expected Sn window contains two dominant phases, a scattered P wave with a v_h around 7.1 km/s and a mantle shear wave with v_h of 4.8 km/s. The *Lg* waves are coherent between 0.5 and 2.0 Hz, with a dominant v_h of 4.2 km/s. The Rg wave at frequencies between 0.5 and 0.8 Hz is dominantly composed of a coherent fundamental mode Rayleigh wave with a v_h of 3.0 km/s. At higher frequencies (>0.8 Hz), this coherent Rayleigh wave is not observed in the Rg window due to attenuation during wave propagation.

The difference between the phase velocities of Lg and Rg implies that the dominant waves composing Lg and Rg are originated differently in the source region. The dominant wave field in the near source region that eventually becomes regional Lg wave is coherent and has an *SmS*-type of slowness. If a near source Rg-to-Lg scattering is primarily responsible for the Lg excitation, we are expected to observe either a strong peak in the FSPS concentrated near the Rg slowness (slower than 3.0 km/s at frequencies higher than 0.8 Hz), or multiple peaks in the FSPS with reduced amplitudes. The former FSPS pattern is observed if the scattered Rg wave exists in a form of a plane wave in the near source region. The latter pattern is expected if the scattered Rg waves exist in a form of non-planar waves or multiply superposed plane waves. Neither of the two patterns are observed. We therefore infer that for our data set, a Rg-to-Lg scattering does not seem to dominate the Lg excitation process. It is also found that the strength of shear waves contained in the expected Sn window varies with local geology much more than does the strength of Lg. Since the Sn is enriched in its high-frequency (>1 Hz) content as compared to the Lg, this observation suggests that the local geology influences shear wave excitation at high frequencies more than at lower frequencies. We plan to investigate the spectral characteristics of regional wavefields from UNEs of various test sits to infer the best-fit source model.

OBJECTIVES

The objective of this research project is to understand how regional P (Pn, Pg) and S waves (Sn, Lg) are generated by UNEs using regional clustered UNEs that were recorded at single stations. The single-station records can be treated as array records under a reciprocal theorem. Hundreds of clustered UNEs in central Asia and Nevada between the 1970s and 1990s were recorded at common regional stations. The waveforms of the source array records provide dense time-space domain sampling of the wavefields in the near source region.

A FSPS analysis is applied to the source-array records to explore the phase composition of regional waves from UNEs as they leave the sources. In each frequency band we estimate the powers of various wavelets, including direct body and surface waves and scattered/multipathed waves. Improved depth and yield estimates can be determined in the course of the study. In the next stage, we examine whether each previously proposed mechanism for regional wave excitation is compatible to observed phase composition. Best-fit or dominant excitation mechanisms and best-fit spectral models for regional waves from UNEs will be presented. Using the best-fit models, we shall develop scalings of these parameters with event magnitudes and depths, and explore the dynamic relations among all these parameters and testing styles, local structures, and geological environments.

RESEARCH ACCOMPLISHED

Under a reciprocal theorem, velocity seismograms from these clustered explosion sources can be treated as seismograms at an array of fictitious strain meters buried at the source locations, recording a single force acting at the station location [Spudich and Bostwick, 1987; Xie et al., 1996]. We apply a frequency-wave number technique to the source array seismograms, and investigate the phase composition of regional waves recorded at the BRV in Kazakhstan as they leave the source region.

Data acquisition and assembly of ground truth information

Short-period displacement records at BRV for UNEs at the Balapan nuclear test site between 1968 and 1989, are analyzed and shown in Figure 1. The sampling intervals of the data are 0.032 s and 0.096 s . The records display high signal-to-noise ratios (S/N>50 dB) between 0.5 and several Hz. The epicentral distances vary between 680 and 697 km. The event magnitudes (m_b) are between 4.8 and 6.2, with 58 out of the total 67 events having magnitudes larger than 5.5 (Marshall et al., 1985; Kim et al., 2001). High-precision hypocentral locations of the UNEs are measured geodetically, with uncertainties of less than 200 m (NNCRK, 1999; Thurber et al., 2001). Precise ("ground truth") origin times and depths of burial are available for 10 UNEs between 1985 and 1989 (Adushkin et al., 1997). For all UNEs, teleseismically determined origin times are also available from multiple sources, such as the International Seismological Centre (ISC) and Thurber et al. (2001).

Estimation of scaling relationships among depth, yield, and magnitude

Groundtruth information on the depths and origin times of most Balapan UNEs are not available. To estimate the depths of the UNEs used in this research project, we calibrate the scalings among the body-wave magnitudes (m_b), the yields in kilo-ton (Y), and the depths in meter (H) of those Balapan UNEs whose ground truth depths and/or yields are available. These scalings are then used to estimate H values of all other events from their m_b values. Several authors [e.g., Bocharov et al., 1989; Spivak, 1996; Adushkin et al., 1997 information presented at Seismological Society annual meeting, April, 1992] provided Y and m_b values of 19 Balapan explosions. The magnitudes (m_b) of Balapan nuclear explosions are given in Marshall et al. [1985] and Kim et al. [2001]. Using these values we obtain a relationship (Figure 2)

$$m_b = 0.753 \cdot \log(Y) + 4.428. \qquad (1)$$

This relationship is very similar to that obtained by Ringdal et al. (1992).

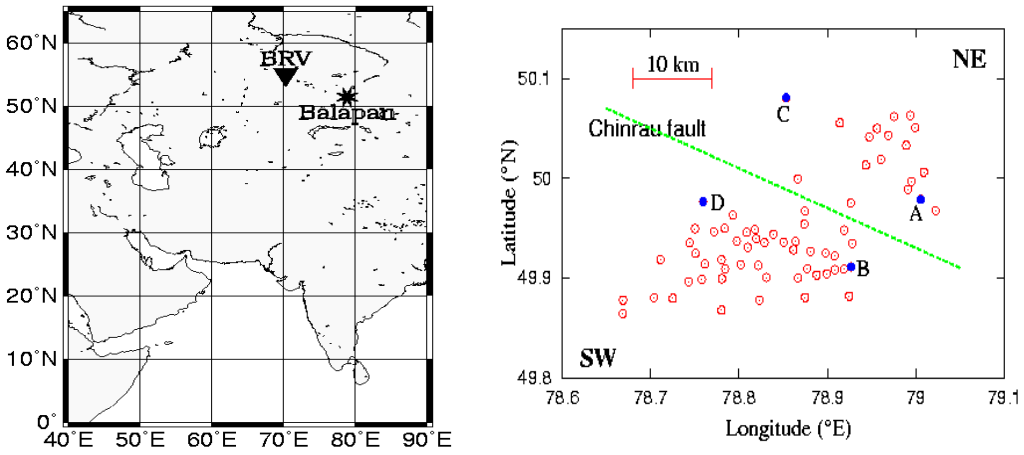

Figure 1. Maps showing locations of the Borovoye observatory (BRV) and the Balapan nuclear test site (left), and locations of nuclear explosions in the test site (right). The explosion sources can be grouped into NE (18 events) and SW subregions (49 events) according to the velocity and geological structure. The dotted line dividing the Balapan region approximately delineates the Chinrau fault. Time records from four representative events (A,B,C,D) are given in Fig. 7.

An empirical scaling between the yield and depth of burial is given in a form of cube-root rule in the Balapan test site [Khalturin, 2004, personal communication; also cf. Lay et al., 1984]:

$$H = c \cdot \sqrt[3]{Y}, \qquad (2)$$

where H is the depth of burial in meters and c is a constant . Thus, using the given scaling relationships and available groundtruth values of H, we estimate the scaling relationship between m_b and H by

$$m_b = 2.25 \cdot \log(H) - 0.10. \qquad (3)$$

From the m_b-H relationship, we calculate the unknown depths of burial.

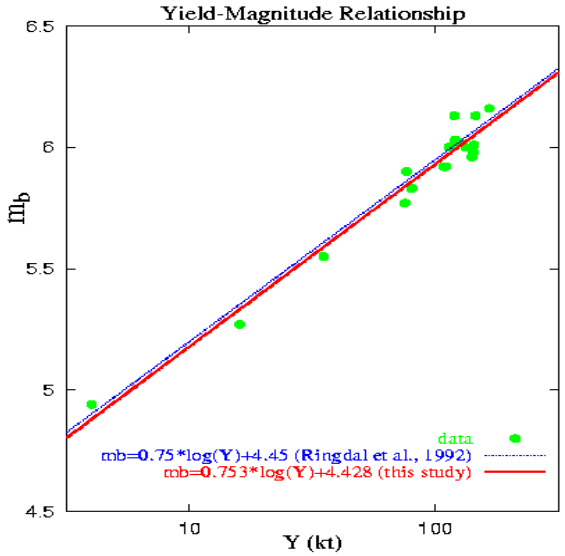

Figure 2. A linear relationship between yield (Y) and body-wave magnitude (m_b) obtained in this study. The refined relationship is very close to the previous result of Ringdal et al. (1992).

Frequency-slowness power spectra (FSPS) analysis

We analyze FSPS of source-array records using a conventional frequency-wave number (F-K) technique to study the phase velocities of the waves in source region. In the original (true) geometry, the analysis yields the phase composition of the wavelets leaving the explosion sources. The slowness power spectrum (P_c) at angular frequency ω and wave number **k** (= ω**s** , where **s** is the slowness vector) is determined by

$$P_c(\omega\mathbf{s},\omega) = \left|U(\omega\mathbf{s},\omega)\right|^2, \qquad (4)$$

where U is the double-Fourier transform of the waveforms $u(\mathbf{r},t)$ recorded at location **r** in the reciprocal geometry. When a seismic wave is approximately nondispersive in a finite frequency range, coherent power spectral features can be enhanced by stacking the $P_c(\omega\mathbf{s}, \omega)$ over frequencies (ω) [Spudich and Bostwick, 1987]:

$$P_w(\mathbf{s}) = \frac{1}{N}\sum_{j=1}^{N} P_c(\omega_j\mathbf{s},\omega_j)\cdot\frac{1}{m_j}, \qquad (5)$$

where N is the number of discrete frequencies, ω_j is the jth angular frequency, P_W is the stacked slowness power spectrum, and m_j is a normalization (whitening) factor. P_W indicates the relative strength of a plane wave leaving the source region in a finite frequency range. The pre-whitening normalization removes the effect of non-flat responses of the instrument and wave propagation [Spudich and Bostwick, 1987] which are virtually the same for all records.

Phase composition

We do FSPS analysis on a slowness-azimuthal angle domain with a discrete slowness interval of 0.05 s/km and a discrete azimuthal angle interval of 1°. In Fig. 3, the slowness power spectrum of Pn waves has a maximum value at horizontal slowness (s_h) of 0.125 s/km, which corresponds to P waves travelling in the uppermost mantle with a phase velocity (v_h) of 8.0 km/s [Quin and Thurber, 1992]. For the Pn phase velocity, the uncertainty introduced by the discrete domain is ±0.17 km/s. The azimuth of the maximum power is 303° which agrees with the great-circle azimuths of events (302.2° - 304.5°).

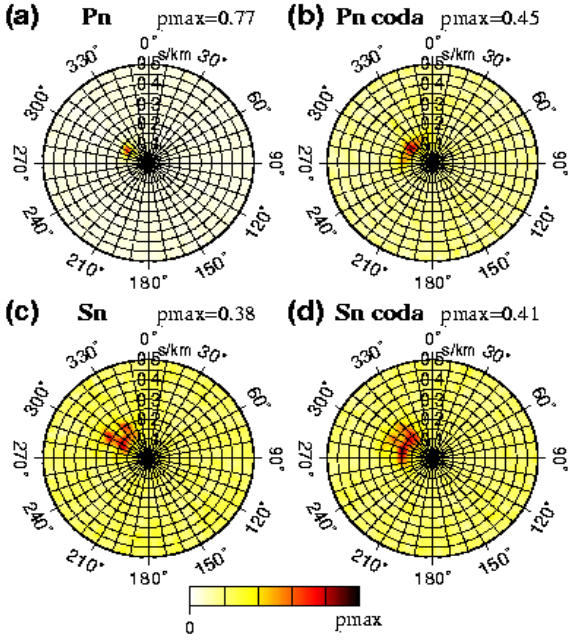

Figure 3. Slowness power spectra of (a) Pn, (b) Pn coda, (c) Sn, and (d) Sn coda. The event lapse-time windows for Pn, Pn coda, Sn, and Sn coda are 92 to 96 s, 125 to 130 s, 162 to 170 s, and 178 to 186 s, respectively. The frequency band used is 0.5 to 3.0 Hz. The annotation of pmax refers to the maximum power shown in the individual plot. This corresponds to the "pmax" shown in the color bar of the figure.

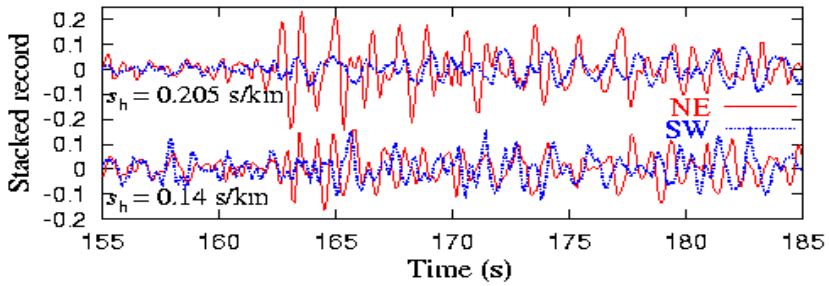

Figure 4. Slant-stacked seismograms of Sn window along horizontal slowness (s_h) of 0.205 and 0.14 s/km that are two dominant phases in the window. The stronger Sn at the NE subsite is mainly caused by enhancement of the phase with an s_h of 0.205 s/km.

The slowness power spectrum of the expected Sn window, which spans group velocities between about 4.0 and 4.3 km/s, exhibits two dominant phases with s_h of 0.14 and 0.205 s/km, respectively (Fig. 3(c)). The phase with s_h of 0.14 s/km (v_h=7.1 km/s) spreads into multiple azimuths, implying that it is composed of multiple forward scattered lower crustal (Pg) waves. The phase with s_h of 0.205 s/km (v_h=4.8 km/s) is the shear wave propagating in the uppermost mantle. The scattered Pg phase displays a comparable energy level to the Sn phase (Fig. 4). This implies that a strong lateral velocity heterogeneity or topography variation must be present along the Pg ray path in the near source region. The complexity of Sn phase is discussed more in a following subsection.

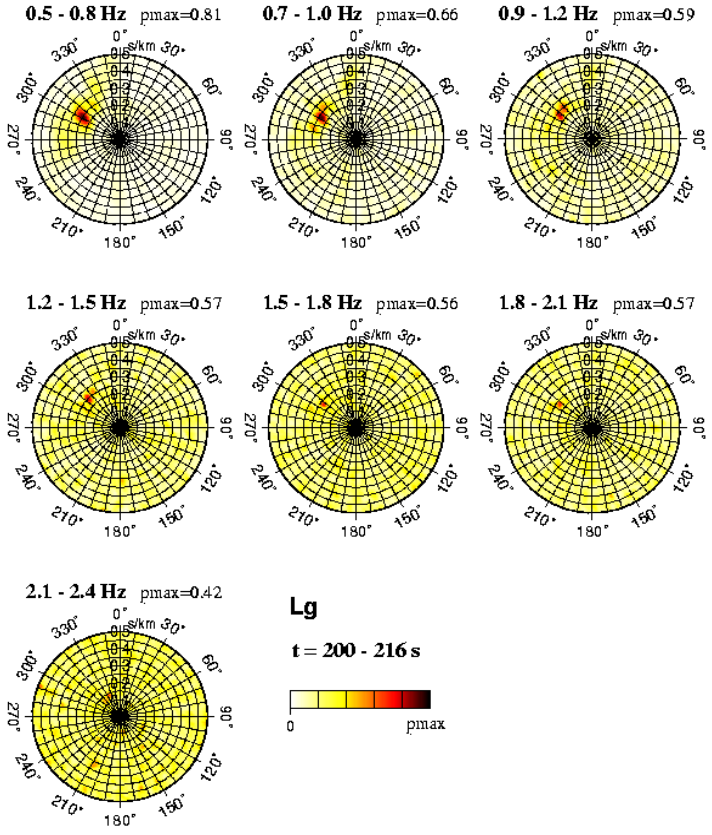

Figure 5. Slowness power spectra of the Lg window in various frequency bands. The dominant phase with phase velocity of 4.2 km/s is observed in frequency range between 0.5 and 2.0 Hz, above which the coherency in slowness power spectra degrades.

The phase velocities of Pn and Sn coda are similar to those of Pn and Sn (Figure 3). But, the azimuthal distributions of the maximum slowness power spectra of the coda are wider than those of the Pn and Sn . This indicates that the waves constituting the coda tend to undergo forward scattering in the near source region. The azimuthal span of slowness power spectra of coda increases with time, indicating that the scattered rays tend to increasingly deviate from the great-circle azimuth toward later coda.

The Lg waves are composed of crust-guided shear waves, with group velocity of 3.0 to 3.6 km/s [e.g., Kennett, 2002]. The dominant phase in the expected Lg window has a v_h of 4.2 km/s at frequencies up to 2.0 Hz (Fig. 5). This phase velocity is typical of Lg observed in conventional receiver array analysis [e.g., Der et al., 1984]. The coherency of the phase in the Lg window degrades at frequencies above 2.0 Hz.

In time window where fundamental mode Rayleigh (Rg) wave is expected, the dominant signal frequency is around 0.2 to 0.8 Hz. The dominant phase velocity in that window is 3.0 km/s at frequencies between 0.5 and 0.8 Hz, and appears to increase gradually with frequency (Fig. 6); it reaches 4.0 km/s at frequencies between 0.9 and 1.2 Hz, and 5.7 km/s at frequencies between 1.3 and 1.6 Hz. At frequencies above 1.6 Hz, the coherency in the slowness power spectra decrease drastically owing to a lack of coherent high-frequency energy. These observed high phase velocities ($v_h \geq 4.0$ km/s) at frequencies higher than 0.8 Hz are too high for Rg wave. These high phase velocities suggest that the Rg wave is attenuated out at these high frequencies, leaving the dominant signals to be those from forward-scattered higher mode or mantle *S* waves. The absence of Rg at high frequency is confirmed by a multiple filter analysis [Herrmann, 2002].

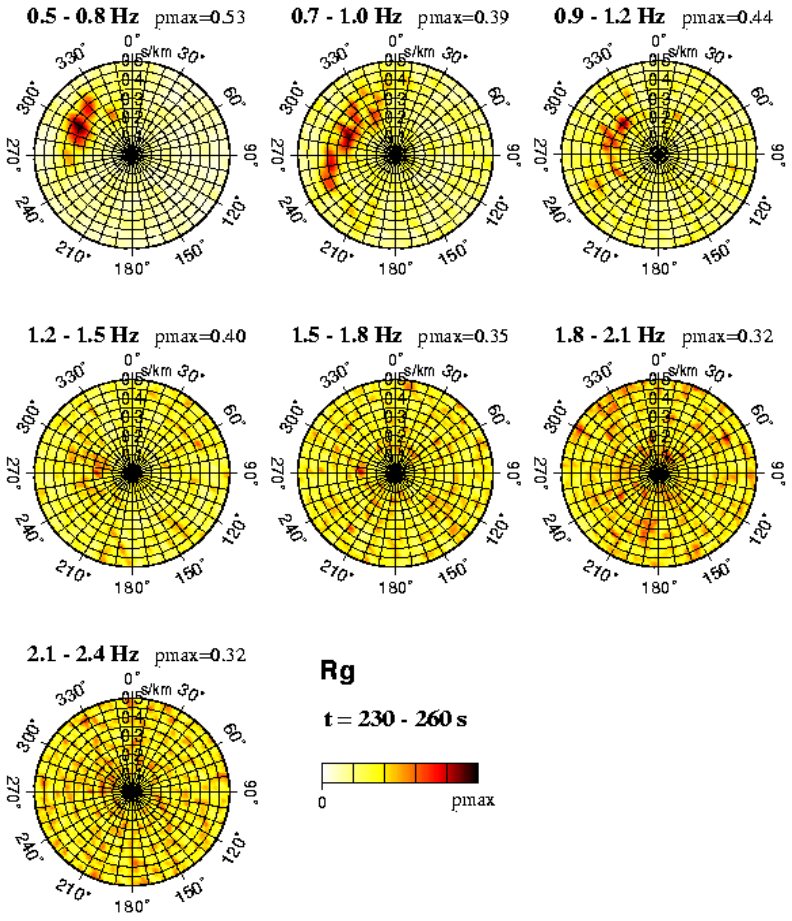

Figure 6. Slowness power spectra of the expected *Rg* window for various frequencies. The phase velocity of Rg is 3.0 km/s at frequencies between 0.5 and 0.8 Hz, which is the dominant frequency range of coherent *Rg* signal. Phases at higher frequencies appear to be scattered Lg and body waves with higher phase velocities. Note the coherency generally degrades with frequency.

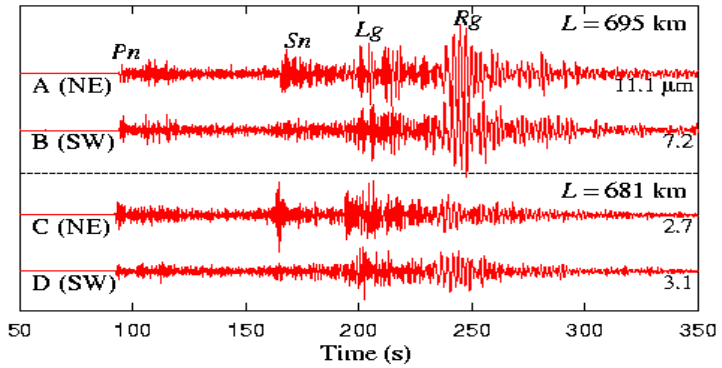

Figure 7. BRV seismograms from four events (A,B,C,D) in Fig. 1 (b). The seismograms are normalized for Lg waves. The reference Lg amplitudes for normalization are presented at the ends of records. Strong Sn waves are observed in the seismograms from the NE subsite that has a slower velocity structure, while the Sn waves are rather weak in the records from the SW subsite with a faster velocity structure.

In Figure 7, we show records at four locations (A, B, C, D in Figure 1(b)) with epicentral distances of about 695 and 681 km. The selected pairs of records are from events with similar magnitudes (m_b): the m_b of A and B are 6.01 and 5.86, and those of C and D are 5.29 and 5.45, respectively. The variation of Rg amplitudes with m_b is obvious in the figure. It is well known that the strength of Rg is dependent on both the size of explosion (m_b) and the depth of burial. In Figure 7, on the other hand, the Lg amplitudes are less variable than the Rg amplitudes.

In a hypothesis that Rg-to-S scattering is a dominant mechanism for Lg generation, Lg is expected to have the same dominant phase velocity as Rg at the same frequencies. If the scattered Rg waves are present in a form of plane waves in the near source, a strong peak in the FSPS concentrated near the Rg slowness should be observed. On the other hand, if the scattered Rg waves exist in a form of non-planar waves or multiply superposed plane waves, multiple peaks with reduced magnitudes in the FSPS are expected. However, we observe that the Lg slowness power spectra is concentrated at a phase velocity of an SmS (v_h=4.2 km/s) in frequencies between 0.5 and 2.0 Hz, while the phase composition in the Rg window varies with frequency. A coherent and dispersive fundamental mode Rayleigh wave with v_h of 3.0 km/s is observed below 0.8 Hz (Figs. 6, 7). The fundamental mode Rayleigh wave is not observed at high-frequencies (> 0.8 Hz) since it is attenuated out during the regional-distance (around 690 km) propagation. The distinct difference in FSTS composition between Lg and Rg implies that Rg-to-S scattering does not appear to be a dominant mechanism for Lg excitation of our data set.

Effects of source site geology on shear waves

We split the data set into two sub-groups according to event locations and local geology (Figure 1(b)). The shear wave velocity of uppermost crust at the NE subregion is about 0.4 km/s lower than the SW subregion (Bonner et al., 2001). We find that the phase compositions from the two subgrouped data exhibit a clear difference in the expected Sn window (Figure 8). The slowness power spectrum for the slower-velocity NE subregion is dominated by a strong shear-wave energy with an s_h of 0.205 s/km. On the other hand, shear-wave energy is relatively weak for the higher-velocity SW subregion. Raw seismograms from the two subregions are compared in Fig. 7. A striking feature is that the records from the NE subregion have strong and impulsive Sn waves, while those from SW region have weak Sn waves (see also, Fig. 8).

We also examine the relative amplitudes of shear wave and scattered Pg waves using a slant-stack technique. We stack the waveforms in the expected Sn window along the two dominant slownesses (s_h) of of 0.14 and 0.205 s/km (Figure 4). The stacked records show that the strong Sn energy from the NE subsite is largely caused by the larger amplitudes of the mantle shear wave propagating with an s_h of 0.205 s/km. On the other hand, the amplitude of the shear wave from the SW subsite is weaker as it becomes comparable to that of the scattered Pg wave with an s_h of 0.14 s/km.

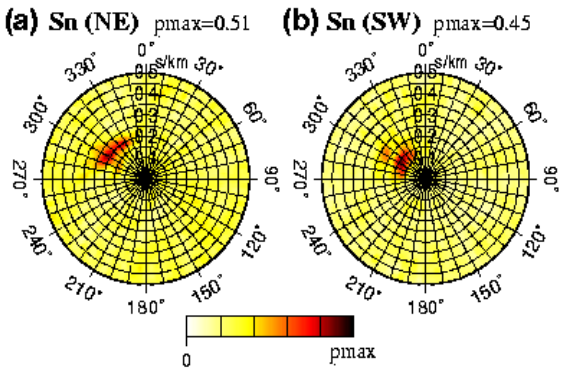

Figure 8. Slowness power spectra of the expected *Sn* window for data sets from two subsites ((a) NE, (b) SW) which were divided according to the velocity structure. The NE subsite has a lower velocity structure than the SW subsite. The *Sn* window used is between 162 and 170 s. The frequency band used is 0.5 to 3.0 Hz.

The amplitude of the Lg waves is less variable with the source locations than the Sn in Fig. 7. The spectra of Sn are enriched between about 1 and 3 Hz as compared to Lg spectra. Apparent corner frequencies of Sn are 2 to 3 times higher than those of Lg. This is consistent with the substantial report of Xie (2002) that different regional waves exhibit different source corner frequencies from UNEs. These observations suggest that the efficiency of shear wave excitation by UNEs may be dependent on source site geology in a frequency-variable manner: shear wave excitation may be more variable at higher frequencies. This scenario is consistent with a physical consideration that the excitation of shear waves with shorter wavelengths is more affected by the shallow source zone geological structures.

CONCLUSIONS

We investigated the near-source phase composition of regional seismic waves leaving underground nuclear explosions at the Balapan test site by applying a slowness power spectral analysis to source array records under a reciprocal theorem. The dominant Pn phase velocity (v_h) is about 8.0 km/s. The energy in the expected Sn window is composed of scattered crustal Pg wave with a v_h of 7.1 km/s and the mantle shear waves with a v_h of 4.8 km/s. The Lg wave in a frequency range between 0.5 and 2.0 Hz has a phase velocity of 4.2 km/s that is typical for super-critically reflected crustal S waves. On the other hand, the expected Rg window is dominated by a fundamental mode Rayleigh wave with a v_h of 3.0 km at frequencies below 0.8 Hz. Above 0.8 Hz the phase coherency degrades drastically owing to a strong attenuation of Rayleigh wave during propagation. From the comparison of slowness power spectral composition between Lg and Rg, the Rg-to-S scattering mechanism does not appear to be a dominant mechanism for the Lg excitation from Balapan UNEs.

The geology of the source region appears to play an important role on the strength of mantle shear wave in the expected Sn window. In that window, slower near surface velocity in the source region seems to enhance shear waves. On the other hand, the strength of Lg waves is much more robust with varying source region geology. The Lg window generally contains lower frequency content relative to the Sn window. The observation implies that source region geology tends to make stronger influence on the strength of higher-frequency shear waves. The study is currently being expanded to other UNE records (e.g., Delgelen test site records) for comparisons with the observations from the Balapan records.

ACKNOWLEDGEMENTS

We thank Howard Patton, Paul Richards and Bill Menke for fruitful comments on the study, Won-Young Kim for information on data and instrument response, Vitaly Khalturin for information on nuclear explosions at Kazakhstan.

REFERENCES

Adushkin, V. V., V. A. An, V.M. Ovchinnikov, and D.N. Krasnoshchekov (1997), A jump of the density on the outer-inner core boundary from the observations of PKiKP waves on the distance about 6 degrees, *Doklady Akademii Nauk* 354: (3), 382-385.

Bocharov, V. S., Zelentsov, S. A., and Mikhailov, V. I. (1989), Characteristics of 96 underground nuclearexplosions at the Semipalatinsk test site, *Atomnaya Energiya* 67: 210-214, (in Russian).

Bonner, J. L., D. C. Pearson, W. S. Phillips, and S. R. Taylor (2001), Shallow velocity structure at the Shagan River test site in Kazakhstan, *Pure Appl. Geophys*. 158: 2017-2039.

Der, Z., M. E. Marshall, A. O'Donnell, and T. W. McElfresh (1984), Spatial coherence structure and attenuation the *Lg* phase, site effects, and interpretation of the *Lg* coda, *Bull. Seism. Soc. Am.* 74: 1125-1148.

Herrmann, R.B. (2002), *Computer Programs in Seismology*, ver3.30, Saint Louis University.

Kennett, B. L. N. (2002), *The Seismic Wavefield*, Volume II, Interpretation of Seismograms on Regional and Global Scales, Cambridge University Press, New York.

Kim, W.-Y., P. G. Richards, V. Adushkin, and V. Ovtchinnikov (2001), Borovoye digital seismogram archive for underground nuclear tests during 1966-1996, Technical Report, Lamont-Doherty Earth Observatory of Columbia University.

Lay, T., D. V. Helmberger, and D. G. Harkrider (1984), Source models and yield-scaling relations for underground nuclear explosions at Amchitka Island, *Bull. Seism. Soc. Am.* 74 (3): 843-862.

Marshall, P. D., T. C., Bache, and R. C., Lilwall (1985), Body wave magnitudes and locations of Soviet underground nuclear explosions at Semipalatinsk Test Site, *AWRE Report,* No. O 16/84, H.M. Stationery Office, London.

NNCRK (1999), Technical Report, Proceedings of the Workshop on IMS Location Calibration, contributed by the National Nuclear Centre of the Republic of Kazakhstan, Oslo, Jan 1999.

Quin, H. R. and C. H. Thurber (1992), Seismic velocity structure and event relocation in Kazakhstan from secondary *P* phases, *Bull. Seism. Soc. Am.* 82, 2494-2510.

Ringdal, F., P. D. Marshall, and R. W. Alewine (1992), Seismic yield determination of Soviet underground nuclear explosions at the Shagan River test site, *Geophys. J. Int.* 109: 65-77.

Spivak, A. A. (1996), Aftershocks of underground nuclear explosions, *Geoecology* N6: 27-42, (In Russian).

Spudich, P. and T. Bostwick (1987), Studies of the seismic coda using an earthquke cluster as a deeply buried seismograph array, *J. Geophys. Res.* 92: (B10), 10,526-10,546.

Thurber, C., C. Trabant, F. Haslinger, and R. Hartog (2001), Nuclear explosion locations at the Balapan, Kazakhstan, nuclear test site: the effects of high-precision arrival times and three-dimensional structure, *Phys. Earth Planet. Inter.* 123: 283-301.

Xie, J. (2002), Source scaling of *Pn* and *Lg* spectra and their ratios from explosions in central Asia: Implications for the identification of small seismic events at regional distances, *J. Geophys. Res.* 107: (B7), 2128, doi:10.1029/2001JB000509.

Xie, J., L. Cong, B.J. Mitchell, and J.-M. Chiu (1996), Complexities in high-frequency seismic waveforms due to three-dimensional structure in the New Madrid Seismic Zone, *J. Geophys. Res.* 101: (B3), 5751-5778.